Advances in Water Resources 78 (2015) 1–8

Contents lists available at ScienceDirect

Advances in Water Resources

journal homepage: www.elsevier.com/locate/advwatres

Peak and tail scaling of breakthrough curves in hydrologic tracer tests

T. Aquino *, A. Aubeneau, D. Bolster

Department of Civil & Environmental Engineering & Earth Sciences, University of Notre Dame, 46556 IN, USA

ARTICLE INFO

Article history:
Received 5 October 2014
Received in revised form 10 December 2014
Accepted 27 January 2015
Available online 7 February 2015

Keywords:
Anomalous transport
Breakthrough curves
Particle tracking

ABSTRACT

Power law tails, commonly observed in solute breakthrough curves, are notoriously difficult to measure with confidence as they typically occur at low concentrations. This leads us to ask if other signatures of anomalous transport can be sought. We develop a general stochastic transport framework and derive an asymptotic relation between the tail scaling of a breakthrough curve for a conservative tracer at a fixed downstream position and the scaling of the peak concentration of breakthrough curves as a function of downstream position, demonstrating that they provide equivalent information. We then quantify the relevant spatiotemporal scales for the emergence of this asymptotic regime, where the relationship holds, and validate our results in the context of a very simple model that represents transport in an idealized river.

1. Introduction

Rivers are the backbone of environmental flows. Distilled rain water acquires dissolved solutes and suspended particulates as it travels on hill-slopes. This water discharges into the river network, where it travels over considerable distances as rivers link landscapes over continental scales [31]. Rivers also act as filters by processing and transforming the load they carry, influencing the biogeochemistry of downstream water bodies [35]. Thus, understanding the processes responsible for the physical translocation and the biogeochemical transformations of upstream inputs to downstream outputs is critical to scientists, stakeholders and decision makers.

Streams and rivers are complex, heterogeneous systems, with fast surface flow transporting substances quickly in the main channel and slow boundary layer and subsurface flow retaining substances for potentially long periods of time. This broad separation of velocities and associated time scales leads to anomalous transport, which cannot be adequately described with traditional one-dimensional Fickian advection dispersion models [33]. The trapping of solutes in a river's bed-sediment leads to heavy-tailed residence times which manifest as power law tails in experimental breakthrough curves (BTCs) [25]. These heavy tailed BTCs demonstrate long-term retention of solutes in rivers, which is particularly important for the many biogeochemical processes that occur in the slow regions near or inside the river-bed [6,16,26,34].

In traditional tracer tests, a pulse (or drip) of tracer is released and its concentration over time is measured at some downstream location(s) to obtain BTCs. The mass of stream-borne dissolved solutes entering the bed is often only a small fraction of the total mass and it is further diluted upon return to the open channel. The signals associated with tracers that have traveled through the bed therefore appear at very low concentrations in measured BTCs, often orders of magnitude below peak concentrations [21]. This poses a significant experimental challenge as reliable and sufficiently sensitive measurements can be difficult to obtain. Typical methods based on electric conductivity resolve only 2 to 3 orders of magnitude, while fluorescent dies can resolve over 4 orders of magnitude. Even though isotopic tracers can be very sensitive, up to 6 orders of magnitude for stable isotopes and 8 or 9 for radioactive tracers, they are seldom used and most experiments only resolve relatively short timescales [14,40]. Conversely, the peak concentration of a BTC from a pulse injection is a reliable measurement, because it is typically much larger in magnitude. The change in peak concentration with downstream distance could therefore provide reliable evidence of anomalous transport characteristics.

Any apparent mass loss in the BTC of a conservative tracer must have been retained during transport and should eventually leak back to the main flow. This would be true for example in flumes, or rivers on bedrock without connection to a regional aquifer. Even when there are gains and losses through groundwater exchange, this concept remains valid so long as a proper mass balance is enforced [17]. The mass lost from the BTC compared to the mass actually injected upstream (ignoring the flowpaths bypassing the sampling location) should thus reappear as a tail if the instruments have sufficient sensitivity and sampling occurs over sufficiently long times. We argue that a dynamical relationship therefore exists between the bulk of the solute, which is transported directly by the water column in the river, and the solute mass that reenters the

* Corresponding author.
E-mail address: tdecampo@nd.edu (T. Aquino).

http://dx.doi.org/10.1016/j.advwatres.2015.01.016
0309-1708/

water column after being retained in the sediment bed. If we consider a BTC measured at a fixed location, the fraction of solute that has spent a considerable time in the sediment bed will define the long-time tailing behavior. Since the mass recovered in the tail was "lost" from the main channel flow, one should expect an equivalent signal missing from the main pulse, which in turn should also appear as a faster than expected decay in the peak of the BTC downstream [4]. Thus, if we consider multiple BTCs measured at different downstream positions, we may ask the following question: Given the behavior of the peak value of the BTCs at multiple positions, can we infer the tailing properties of a single BTC at a fixed position? This idea is illustrated in Fig. 1. A relationship of this type would allow one to infer details about the solute transport occurring in the sediment bed from measurements of the bulk mass transported in the water column. This would provide an alternative method to assess the behavior of BTC tails through measurements of peak concentrations.

The present work is structured as follows. Section 2 presents our model: we derive a general late-time relation between the scaling of the tail of a BTC for a conservative tracer at a fixed downstream position and the scaling of the BTC peak as a function of downstream position. Section 3 is dedicated to illustrating the general results of Section 2 in a concrete scenario, so as to clarify the roles of the underlying physical processes. For this purpose, in Section 3.1 we construct a very simple conceptual model for river transport, which is deliberately chosen to be simple, yet complex enough to demonstrate the desired behaviors. We then determine the relevant spatiotemporal scales for the onset of the asymptotic scaling behavior in the context of this model, and also discuss the pre-asymptotic regime. We validate our results using numerical particle tracking simulations in Section 3.2. An overall discussion is presented in Section 4.

2. Asymptotic behavior of tail and peak scaling

In order to address the question of the relationship between peak and tail scaling in BTCs, it is necessary to describe solute transport in a sufficiently general framework that allows the relationship between retention in the sediment bed and transport in the water column to come to light. Particle-based random walk methods, whether from a theoretical or numerical (particle tracking) perspective, have been used extensively to represent solute transport in flows across a diverse range of hydrologically relevant flows [27,37]. In particular, the related idea of subordination has been used to derive results on peak, tail and moment properties of BTCs for solute transport in heterogeneous porous media [5]. The basic premise of particle-based methods is to discretize the solute plume into a discrete number of individual particles, each of which then move based on probabilistic rules that aim to capture microscopic and macroscopic processes of the system of interest in an effective manner. It is important to note that these pseudo-particles are abstract theoretical (or numerical) devices and do not aim to represent actual individual solute particles [10,15]. They are characterized by effective properties that depend on the specific solute, flow and background medium. These particles are tracked as they move due to advection by the background flow and dispersion according to an appropriate stochastic process representing the dispersive properties of the solute in a particular medium. From a numerical standpoint, particle tracking methods have the benefit of being essentially free of numerical dispersion [13]. From both the numerical and theoretical point of view, these methods provide a very flexible framework to represent transport phenomena, ranging from classical (Gaussian) advective–dispersive transport [28] to more general processes [8,9]. The present work builds on this type of approach to explore peak and tail scaling properties in the context of river and stream transport. Importantly, these methods take into account stochastic properties in a natural fashion. Furthermore, they allow us to derive our results without the necessity of imposing overly restrictive assumptions on the nature of the transport, and they can thus be applied to a variety of natural systems.

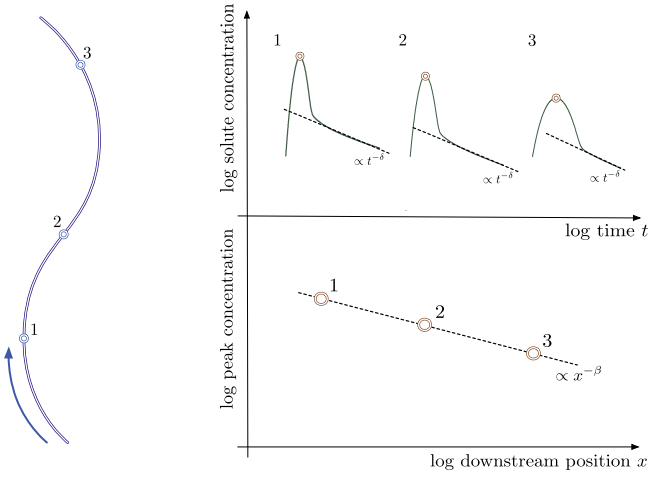

Fig. 1. Given the behavior of the peak value of the BTCs measured at multiple downstream positions (decay exponent β), can we infer the tailing properties in time of a single BTC at a fixed position (decay exponent δ)? Given a number of stations positioned at different downstream positions along a river or stream (left panel), the temporal tail scaling at each position is expected to follow some power law scaling $t^{-\delta}$ at late times (top right panel). We ask the question of whether this behavior has a discernible signature in the peak decay as a function of downstream position, where we expect some asymptotic power law scaling $x^{-\beta}$ (bottom right panel).

2.1. Theoretical framework

In classical random walk approaches, time is discretized and all particles move over a fixed time step according to specific stochastic transport process (e.g. Brownian motion [36], Fickian dispersion [37]). For our theoretical description, we adopt an alternative view often called the continuous time random walk [9] whereby we fix a specified spatial distance along the downstream dimension rather than fixing the time step. We then ask: what is the probability that a particle takes a certain amount of time to traverse this fixed length? In this description, the randomness in the movement of the particles is encoded in the density of waiting times needed to traverse this fixed length. For example, when modeling river transport, a particle that travels through the water column will take a much shorter time to travel a fixed distance than one that is retained in the sediment bed and later released back into the main channel. Similar approaches, where a random process is modified by some waiting time distribution that characterizes an inactive or immobile phase, can be found in [5,8], which rely more explicitly on the related concept of subordination. An overview of the related approaches of fractional advection–dispersion, subordination and continuous time random walks can be found in [33]. To our knowledge, the approach presented here is new in the context of river and stream solute transport and provides a clear picture of the physical processes and assumptions involved.

Let us formalize our ideas. We wish to describe the motion of a particle of solute undertaking random motion starting from a known position x_0 at time t_0. Let x be position downstream, and start by fixing a length l. Assuming that we are interested in length scales over which the movement of a particle is independent of previous history, we can describe the motion of our particle by:

$$\begin{cases} x_{i+1} = x_i + l, \\ t_{i+1} = t_i + \tau_i(l), \end{cases} \tag{1}$$

where the random time increments $\tau_i(l)$ are independent and identically distributed (i.i.d.). We denote their common density by $p_\tau(\cdot, l)$, where l is our fixed characteristic jump length. This process should be interpreted in the following way. The ith occurrence for a particle to travel a distance l downstream takes a time described by a random variable τ_i, which depends only on the jump length l. Since the time increments are assumed i.i.d., $p_\tau(\cdot, l)$ is the first passage time density for a particle starting from position $x = 0$ to reach $x = l$. In this model, all the particles are assumed identical and independent (i.e., they do not interact with each other). Again, alternative descriptions exist for this system, such as the more classical approach implemented in the particle tracking scheme discussed in Section 3.2, or models that include correlation effects between successive particle jumps [11,18,29,30]. However, the current description provides a useful framework for deriving the analytical results that will be discussed in this section.

Consider the process defined by (1). Regardless of the particular path taken by a solute particle, the time it takes to reach n times the characteristic length l downstream for the first time is the sum of n independent random variables, each distributed according to $p_\tau(\cdot, l)$. Since the density of the sum of independent random variables is the convolution of the variables' densities [22], we can write for the random time it takes a particle to reach the downstream position $x = nl$:

$$t_{fp}(x) = \sum_{i=1}^{n} \tau_i(l) \sim p_\tau^{*n}(\cdot, x/n), \tag{2}$$

where p^{*n} denotes the convolution of p with itself n times, and $Y \sim p$ denotes that the random variable Y is distributed according to the probability density p.

Now if the waiting time densities are determined by the same physical processes for arbitrarily small scales, then up to rescaling and centering the $p_\tau^{*n}(\cdot, l)$ are the same. In other words, for two different values of n_1 and n_2, we can shift and rescale x by two constants a and b, such that $p_\tau^{*n_1}(x, l) = p_\tau^{*n_2}(ax + b, l)$; the densities represent the same physics as manifesting at different scales. Recall from the Central Limit Theorem that a large number of finite-variance independent random variables sum to a random variable with a Gaussian density. This is in essence the foundation of Fickian diffusion/dispersion models [36]. In the same manner, by the Generalized Central Limit Theorems, the sum of independent random variables with infinite variance resulting from heavy tails (i.e., exhibiting slower-than-exponential decay, as power laws with decay exponents between 0 and 2) converge to a family of densities called stable densities (see e.g. [22,32]). Under these conditions, the increments of the stochastic process t_{fp} (representing the random time it takes to reach the downstream position x) have a stable density, and t_{fp} is called a stable process. Furthermore, assuming the heavy tails of the waiting times are due to heavy-tailed retention times in the sediment bed, the stable density will exhibit that same tailing behavior for large time. The main significance of the density of the first passage time $t_{fp}(x)$ for BTCs will become apparent in the following section.

Naturally, for every physical system there must exist a scale below which these assumptions do not hold. However, consider l_0, a spatial averaging scale, large enough that all physically relevant processes are captured, and $l \gg l_0$. Then, the number of terms n in the convolution above can be made large, and we may expect the density $p_\tau^{*n}(\cdot, l)$ to be well approximated by a stable density. In what follows, we will assume l can be chosen large enough so that this property holds, and omit the l-dependency in p_τ. In fact, the assumption of independent increments already implies that the length scales in question must be larger than the correlation length of the system [30]. We note, however, that the assumption of a stable process is quite strong, and is at the root of the necessity for a large "basic" scale l_0 above which the theory becomes valid. We postpone the discussion of identifying the relevant scale l to Section 3.1.

2.2. Breakthrough profile and scaling relation

The precise definition of a BTC – i.e., what is actually measured in the field *vs.* what is measured in numerical experiments or predicted by theory – has been discussed in the literature [2]. Depending on the specific measurement techniques employed, care has to be taken to ensure correct comparison between theory and experiments. In order to proceed with our discussion of tailing properties of BTCs, let us first define a BTC in a rigorous way in the context of our mathematical framework.

Consider particle motion as defined by (1). We consider for simplicity that the particles either move downstream (the x-direction) with an x- and time-independent downstream velocity $v(y, z)$ or are effectively immobile. This is a reasonable approximation in the typical scenario where Darcy flow in the sediment bed is much slower than the flow in the water column. Furthermore, we are interested in systems which are typically advection-dominated at the scales of interest. In this context, advection-dominated flow refers to the idea that the width of the peak of a BTC, that is some characteristic dispersive scale, at a downstream scale x of interest is negligible compared to the downstream distance itself. This is quantified by a high Peclet number, defined in terms of the downstream spatial scales of interest and transverse dispersion in the water column; i.e. $\mathrm{Pe} = \bar{u}x/D$ where u is the mean velocity, x is the downstream distance where the BTC is measured and D is a characteristic longitudinal dispersion coefficient. In this case, diffusive fluxes may be neglected and the first passage time through $x = nl$ is proportional to the advective flux of mass through x (that is, through the plane parallel to the yz axes at $x = nl$).

Consider an instantaneous, cross-sectionally homogeneous injection of a tracer at the upstream position $x = 0$ when $t = 0$. With $\check{C}(x, y, z, t)$ the three-dimensional concentration profile at (x, y, z) and time t (physical units of mass per unit volume), the flux of mass through $x = nl$ (units of mass per unit time) is given by:

$$F(x, t) = \int_{A_x} v(y, z)\check{C}(x, y, z, t)\, \mathrm{d}A, \tag{3}$$

where the integral is over the plane through x discussed above. In words, the mass flux through a station located at x is the result of the advection of solute concentration by the water column velocity. We can now define a cross-section-averaged concentration profile, that is a one-dimensional concentration (units of mass per unit length), as:

$$C(x, t) = \frac{F(x, t)}{\bar{v}}, \quad \bar{v} = \frac{\int v(y, z)\, \mathrm{d}A}{A}. \tag{4}$$

For each value of x, $C(x, t)$ represents the BTC at that downstream position. Here $\bar{v}$ is a cross-section-averaged water column velocity, and A is the cross-sectional area of the river, which must not change appreciably along the downstream direction since we have assumed independence of the flow on x. Thus, for each given location downstream x, our BTC definition encodes the cross-sectionally averaged concentration that should be measured at a station at that location as a function of time. This concentration is a result of the mass of solute flowing by the station through the water column. In practice, the experimental measurements of $C(x, t)$ typically rely on a measurement at a single height that is assumed to be representative due to cross-sectional turbulent mixing [39].

For the case of a conservative tracer, all mass will eventually flow past any downstream point, so p_n integrates to unity for each n. Then the breakthrough profile at $x = nl$ can be expressed as:

$$C(x,t) = \frac{M_0}{\bar{v}} p_n(t), \tag{5}$$

where the initial mass of tracer M_0 satisfies for all x:

$$M_0 = \int F(x,t)\mathrm{d}t = \bar{v} \int C(x,t)\mathrm{d}t. \tag{6}$$

Eq. (5) shows the intimate relation between BTCs in advection-dominated flows and the waiting times of our modeling framework. The intuitive interpretation is straightforward: If advection downstream dominates, then the flow past a certain station is predominantly due to particles reaching the station for the first time, so that the concentration can be inferred from the first passage time of the solute to that location. Note that, in our description, each particle in the solute plume is taken to have a first passage time density to $x = nl$ given by p_n, and that the large number of particles comprising the plume essentially sample this density, so that the BTC reflects p_n.

Now we turn back to the assumption of a stable process, as discussed above. In this case, due to the properties of stable densities, the first passage time to a location n segments of length l downstream is completely determined by the first passage time density across a single segment of length l. Mathematically from (2) and the discussion thereafter [22]:

$$p_n(t) = n^{-1/\alpha} p_\tau\left(n^{-1/\alpha}(t - \gamma(nl))\right), \tag{7}$$

where $0 < \alpha \leqslant 2$, and the function γ is determined by the particular stable density followed by the single-segment first passage time density p_τ. For the case of finite-mean waiting times ($1 < \alpha < 2$), we have simply $\gamma(nl) = n\mu$, where μ is the mean of p_τ. However, for $0 < \alpha \leqslant 1$ (which will be seen to apply to the simple case discussed in the next Section), this relation does not hold since the mean becomes infinite. The parameter α defines the scaling of the tail, which decays like $t^{-(\alpha+1)}$. Substituting this result into Eq. (5) we find:

$$C(x,t) = \frac{M_0}{\bar{v}} \left(\frac{x}{l}\right)^{-1/\alpha} p_\tau\left(\left(\frac{x}{l}\right)^{-1/\alpha}[t - \gamma(x)]\right). \tag{8}$$

From this central result we can now extract information about tail and peak behavior. Defining $\eta = \max p_\tau$ and t^* such that $\eta = p_\tau(t^*)$, the value of the peak of the BTC is given by:

$$C_p(x) = \frac{\eta M_0}{\bar{v}} \left(\frac{x}{l}\right)^{-1/\alpha} \tag{9}$$

and it occurs at time:

$$t_p(x) = \left(\frac{x}{l}\right)^{1/\alpha} t^* + \gamma(x), \tag{10}$$

where t^* is the time at which the peak occurs over a single stretch l. Since our waiting time density p_τ falls off at large times like $t^{-(1+\alpha)}$ due to retention in the sediment bed, for fixed x and large times we have from Eq. (8) for late times:

$$C(x,t) \propto \frac{M_0}{\bar{v}} \left(\frac{x}{l}\right)^{-1/\alpha} t^{-(1+\alpha)}. \tag{11}$$

We focus here on the scaling of C_p with downstream distance rather than the time of the arrival of the peak, which depends on the additional function γ. Note that γ need never explicitly be evaluated to obtain this scaling. The key result is that, given a BTC falling of at large times like a power law $t^{-(\alpha+1)}$, the peak concentration exhibits a power law $x^{-1/\alpha}$ for large enough downstream distance x.

We have thus found an answer to our main question, the existence of a relationship between peak and tail scaling for BTCs. We stress again that these results are quite general and independent of the precise details of the transport process taking place in a particular river or stream (so long as power law residence times due to the sediment bed are present). However, measurements have to be taken at a sufficiently large downstream distance, and we have assumed stationarity and homogeneity of the flow along the downstream direction, so that changes in the flow must be negligible over the relevant asymptotic timescales. The necessity of asymptotic scales forcefully arises in the development of an upscaled theory, such as the one presented here, as sampling and scale separation arguments play a fundamental role. In the present model, we require downstream distance x to be greater than the averaging scale l_0 discussed above.

We believe it is instructive to illustrate the application of these results to a concrete simplified case. For that purpose, the next Section is dedicated to the construction of a simple model for river flow, which allows us to illustrate how these scaling properties arise in a particular transport scenario.

3. Particle tracking in a simple river model

In this section, we illustrate the general theoretical results derived in Section 2 in the context of a highly simplified river model based on 2-dimensional open channel flow coupled with a porous substrate. We stress that the aim of the model presented here is not to perfectly represent a real system, but rather to elucidate how the results above can be observed and interpreted in a concrete transport scenario. We have thus constructed a highly idealized model that we believe retains the main ingredients needed to understand the fundamental properties of the BTCs observed in natural systems that our general model aims to capture.

In the context of this model, it is possible to identify the spatiotemporal scales that control the different regimes of peak concentration scaling. This provides us with valuable insights into the physical characteristics that are expected to affect the relevant properties of BTCs in natural systems, and should be seen as a basis for the design and interpretation of experiments using the general framework of Section 2. We first describe the model and then present particle tracking results.

3.1. Model

A schematic of our conceptual river can be found in Fig. 2. The flow is assumed to be gravity-driven, and the fundamental physical parameters are: acceleration of gravity g, slope of the river bed s,

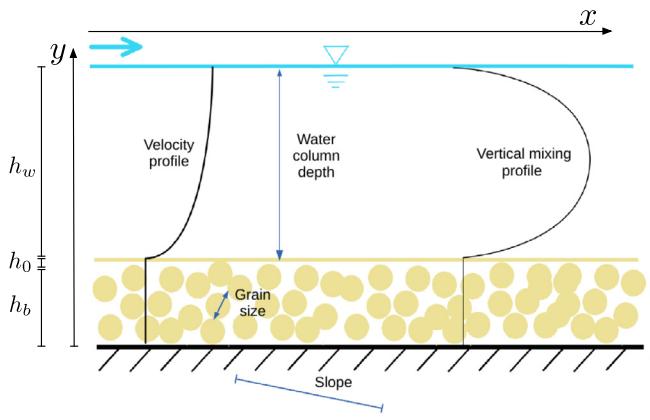

Fig. 2. Conceptual model for river transport. The physical parameters are discussed in the text.

height of the water column h_w, height of the sediment bed (above impervious bedrock) h_b, and sediment grain diameter D_{50}. We consider two-dimensional flow and neglect variations in the remaining transverse direction. A similar model is used in [4].

The flow in the water column is governed by standard gravity-driven open channel flow. The longitudinal velocity profile follows the log law of the wall [24]:

$$u = c_1 \frac{u_*}{\kappa} \log\left(\frac{y - h_b}{h_0}\right) + u_D, \tag{12}$$

where $\kappa \approx 0.4$ is the Von Karman constant, and the dimensionless constant c_1 corrects for effects found in natural systems not accounted for by the theory. The friction velocity is given by:

$$u_* = \sqrt{g h_w s} \tag{13}$$

and h_0 is a roughness height where the flow connects continuously to a standard gravity-driven Darcy flow in the sediment bed. The (longitudinal) Darcy velocity u_D is parametrized as [7]:

$$u_D = c_2 D_{50}^2 s. \tag{14}$$

Here c_2 is a dimensional constant.

The dispersion profile in our model is parametrized so as to account for turbulent mixing effects. Transverse turbulent dispersion in the water column follows a parabolic profile [23]:

$$D_y = c_3 \kappa u_* h_w y'(1 - y'), \tag{15}$$

where $y' = (y - h_b)/h_w$ is a nondimensional height and c_3 is again a nondimensional parameter. Longitudinal turbulent dispersion is parametrized as [24]:

$$D_x = 5.93 h_w u_*. \tag{16}$$

Dispersion in the sediment bed is taken isotropic and parametrized as:

$$D_D = c_4 D_{50} u_D, \tag{17}$$

with c_4 a nondimensional empirical factor.

In order to obtain velocity and dispersion values in line with typical systems, we take the values $c_1 = 0.4, c_2 = 10\ \mathrm{m^{-1}\ s^{-1}}$, $c_3 = 0.1$ and $c_4 = 10$ for our empirical constants. These values were verified by fitting our model to (currently unpublished) real data of conservative solute injections in rivers. The roughness height is taken proportional to the grain size, $h_0 = 0.1 D_{50}$.

We are interested in the behavior of the BTCs when a homogeneous, instantaneous pulse is injected in the water column at some upstream position. Note that, for reasonable values of the physical parameters, it is appropriate to consider the downstream flow in the water column to be advection-dominated at the asymptotic scales of interest, and the Darcy velocity is much smaller than the (average) velocity in the water column, so that residence times in the sediment bed can be thought of as waiting times (see e.g. [8] for a treatment of immobile states in terms of waiting times). Thus, our asymptotic peak scaling results should hold.

Regarding the behavior of the peak of the BTCs as a function of downstream position, we expect two main regimes to take place. Before a significant amount of mass has made its way into the bed and sampled the heavy-tailed waiting time density to make its way back up, the peak concentration should follow a scaling equivalent to transport in the open channel in the absence of a porous bed. Through dimensional analysis, the characteristic timescale for the loss of mass into the bed should be on the order of:

$$\tau = \frac{h_w^2}{\overline{D_y}}. \tag{18}$$

The overbar denotes cross-section averaging over the water column. Now the corresponding spatial scale is:

$$l_0 = \bar{u}\tau. \tag{19}$$

As the transition to the asymptotic regime derived in Section 2 should happen when a significant fraction of the mass has made it into the bed and sampled the corresponding residence time, the scales above should govern the transition from early time scaling to our asymptotic scaling. Essentially, above these scales all the physics have been sampled, and so they set the scale over which the water column can be thought of as mixed, in the sense that the past history of solute found anywhere on the water column cannot be traced back.

In this model, the solute particles in the sediment bed follow Darcy flow and have zero vertical velocity, and thus the waiting time to come back to the water column once the bed has been entered is associated with a regular diffusion process with no mean velocity. The first passage time density for such a process is Inverse Gaussian [22], which is a stable density with $\alpha = 1/2$. Since the tail of our BTCs is governed by the tail of the return time to the water column once a particle reaches the sediment bed, we expect $\alpha = 1/2$ in our asymptotic regime. We also note that at very late times, due to the finite depth of the sediment bed in the model, a cutoff scale should exist. Although we do not consider this effect further, we note that dimensional analysis yields a characteristic time scale for this phenomenon on the order of $\tau_c = h_b^2/D_D$, which is very large for the parameter values considered in results presented in the next section. For the same reason, the cutoff scale is typically not observed experimentally [3].

3.2. Numerical particle tracking results

We implemented the model described in Section 3.1 using a particle tracking scheme. The scheme solves the Langevin equation for our model. In each iteration i, time is incremented by a fixed step Δt, and the position of each numerical solute particle n is tracked according to [19]:

$$\begin{cases} x_{i+1}^{(n)} = x_i^{(n)} + u(y_i^{(n)})\Delta t + \sqrt{2D_L(y_i^{(n)})\Delta t}\,\xi_{i,x}^{(n)}, \\ y_{i+1}^{(n)} = y_i^{(n)} + v(y_i^{(n)})\Delta t + \sqrt{2D_T(y_i^{(n)})\Delta t}\,\xi_{i,y}^{(n)}, \end{cases} \tag{20}$$

where the $\xi_{i,x}^{(n)}$ and $\xi_{i,y}^{(n)}$ are independent random numbers drawn from a standard Gaussian density with zero mean and unit variance, and u, v, D_L and D_T are the local longitudinal and transverse advective velocities and dispersion coefficients, which are evaluated at each particle's position. Note that the variable transverse dispersion in the water column induces an effective vertical solute advection component in the Langevin description, given by Delay et al. [19]

$$v = \partial_y D_y = c_3 \kappa u_* (1 - 2y'). \tag{21}$$

In the sediment bed, the dispersion coefficient is constant and so this effective velocity is zero there. As the initial condition we uniformly distribute a pulse of solute particles along the height of the water column at $x = 0$.

Breakthrough curves at different downstream stations are defined according to Eq. (5). To obtain the flux past a station, we record the mean times of passage for each particle. The mean time is used to account for eventual multiple passages due to dispersion; multiple passages usually occur within a short time window, and taking the average time mimics the averaging process inherent in any real macroscopic measurement.

In Fig. 3 we illustrate the transition from open channel flow scaling to the asymptotic scaling for varying h_w while keeping all other parameters fixed. In the left panel we show the BTCs at

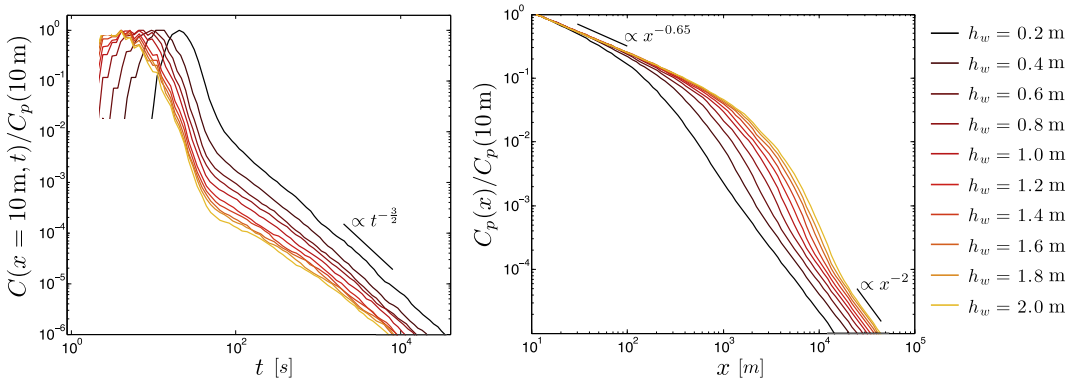

Fig. 3. Breakthrough curves at $x = 10$ m (left), and normalized peak scaling with downstream distance (right) for varying height h_w of the water column. The remaining parameters are $s = 5 \times 10^{-3}$, $h_b = 1$ m, $D_{50} = 10^{-2}$ m. The number of particles used was 2.5×10^5.

$x = 10$ m, normalized to the peak value. The tail scaling follows the expected behavior of $t^{-3/2}$, corresponding to $\alpha = 1/2$. We note here that even at such small downstream distances, where both the advection-dominated flow and the stable process assumptions discussed above are questionable, we still recover the expected tail scaling. In the right panel we show the peak behavior as a function of downstream position. Note that the early regime is well described by a power law with an exponent of approximately 0.65, which is a result of the non-uniform velocity profile in the water column as discussed in more detail below. The transition to the peak behavior anticipated by our model begins at $x = O(l_0)$ for each curve, as predicted in the previous section, and at $x \approx 5l_0$ we obtain the predicted asymptotic scaling of $x^{-1/\alpha} = x^{-2}$. Fig. 4 shows similar results for varying D_{50} with all other parameters fixed. Note that in many cases the scaling in the peak concentration occurs at concentrations that are several orders of magnitude higher than those associated with the tails in an individual BTC, thus highlighting the potential utility of this approach if concentration measurement at lower concentrations is a barrier to identifying these tails.

A discussion of the pre-asymptotic scaling is also in order. For an advection-dominated flow with a uniform velocity profile, the peak scaling corresponding to the regular ADE follows $x^{-1/2}$. However, at short spatial distances our flow is not advection dominated, in the sense discussed in Section 2.2, and the velocity profile is non-uniform. In order to verify that the early $x^{-0.65}$ scaling observed in our particle tracking data is indeed a consequence of these effects, we performed simulations where no sediment bed was present. The results can be found in Fig. 5. We observe the same $x^{-0.65}$ at short distances. At large distances, once the flow

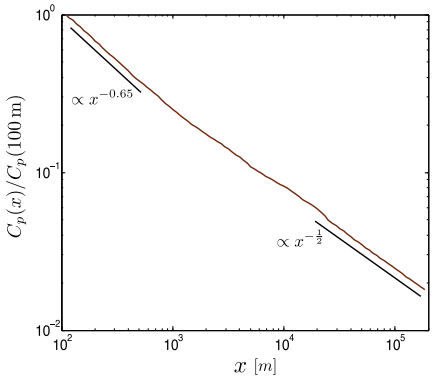

Fig. 5. Normalized peak scaling with downstream distance in the absence of a sediment bed. Parameters are $s = 5 \times 10^{-3}$, $h_b = 1$ m, $h_w = 0.5$ m, $D_{50} = 10^{-2}$ m. The number of particles used was 2×10^5.

can be considered advection dominated and the water column has been well mixed by vertical dispersion, we observe convergence to the standard $x^{-1/2}$ scaling, consistent with the idea of Taylor dispersion at asymptotic times [12,38]. This asymptotic scaling is never observed in our simulations when the bed is present because of the loss of mass into the bed that occurs before this regime emerges.

For the parameters considered here, we find that the transition into the asymptotic peak scaling occurs at a typical distance between 1 – 10 km. We recognize that this length may be very, if not prohibitively, long, but note that other studies also suggest such lengths may be required for proper sampling of all processes

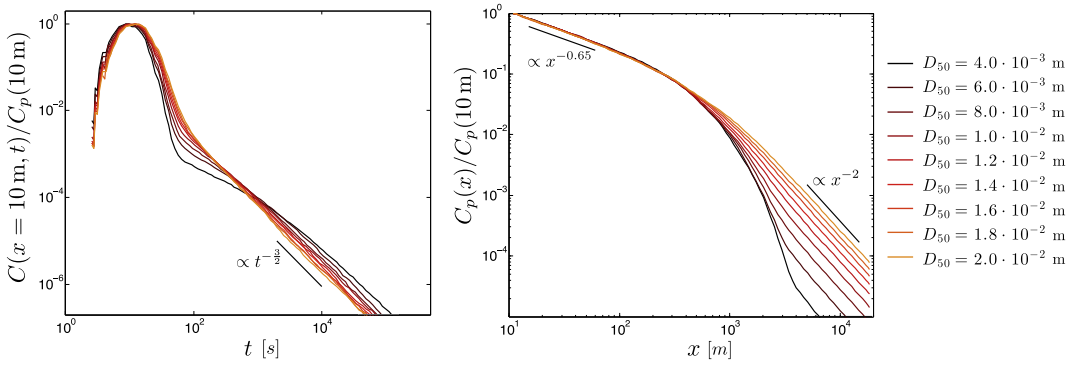

Fig. 4. Normalized BTCs at $x = 10$ m (left), and normalized peak scaling with downstream distance (right), for varying grain size D_{50}. The remaining parameters are $s = 5 \times 10^{-3}$, $h_b = 1$ m. $h_w = 0.5$ m. The number of particles used was 2.5×10^5.

[39]. In practice, it must be remembered that the length scales obtained in this model are illustrative but should not be taken as exact figures, as the precise mechanisms for mixing and solute exchange in natural systems are of course much more complex.

4. Discussion and conclusions

As discussed in the Introduction, measuring the tail scaling for breakthrough curves can be very challenging due to experimental limitations. Here we have addressed the question of whether the interplay between water column solute transport and sediment bed retention can be exploited to obtain a relationship between this tail scaling and the scaling of the BTC peaks, which represent the bulk of the solute mass passing through each location along the river. Our results suggest an alternative method of experimentally determining the tail scaling from peak BTC values measured at different downstream positions. This method is based on a general scaling relation between temporal tail and spatial peak scalings in BTCs measured in river transport.

In Section 2, we obtained the analytical asymptotic scaling relationship through the use of a theoretical random walk framework. This framework allowed us to obtain our results in a general context, so that they should hold in principle for a wide class of natural systems. In Section 3.1 we presented a simple model for river transport. This highly idealized model has the goal of clarifying the role of the basic physical processes involved and illustrating the application of our general results to a concrete case. In the context of this model, we identified the different regimes and respective spatiotemporal scales for the scaling of the peak of BTCs as a function of downstream position. We then saw in Section 3.2 that our theoretical results are supported by numerical particle tracking simulations.

We argue that, although these scalings were derived in the context of a very simple conceptualization of river transport, they identify the fundamental physical mechanisms that underlie the observed behaviors. Thus, they can inform the estimation of the relevant scales for a real system and help design appropriate experiments to validate our results. In particular, we expect that in typical natural systems scaling exponents for the pre-asymptotic and asymptotic regimes described here should have values similar to the ones we obtained, although additional physical properties may lead to different effective solute transport processes and thus different scaling behaviors. Specifically, the pre-asymptotic exponent comes from heterogeneity in the velocity profile, as discussed in Section 3.2, and some deviation from our idealized theoretical profile is to be expected. The asymptotic exponent is determined by α, which originates in residence times in the sediment bed, and thus will depend on properties that impact anomalous transport in the bed (e.g. a sediment bed with fractal structure [1,20]). In an actual experiment, the relevant scales and exponents may be estimated from water column flow data.

We stress the importance of careful analysis of upscaled models such as the one presented here, as they typically require large spatiotemporal limits to be taken. These limitations are often hidden in the mathematics or disregarded in practice. We have shown that the relevant scaling may occur only at a considerable downstream distance. Furthermore, the theory presented here can only be applied when the flow can be approximated as homogeneous and stationary over the relevant spatial and temporal scales, even though it could be generalized to unsteady flows or non-stationary conditions. In particular, large rivers with a deep water column would require long downstream distances that may be unattainable in practice.

Despite these limitations, the present work highlights that there exist alternatives to traditional methods of inferring and measuring anomalous transport. The applicability of each method is dependent on the physical and experimental setup, and careful analysis followed by experiment is necessary to verify and validate modeling strategies.

Acknowledgements

One of the authors (TA) gratefully acknowledges support by the Portuguese Foundation for Science and Technology (FCT) under Grant SFRH/BD/89488/2012. This material is also based upon work supported by the National Science Foundation under Grant Nos. EAR-1344280 and EAR-1351625. The authors also thank Professor Boano and two anonymous reviewers for their helpful comments.

References

[1] Adler P, Thovert J-F. Fractal porous media. Transp Porous Media 1993;13(1):41–78. http://dx.doi.org/10.1007/BF00613270.
[2] Appuhamillage T, Bokil V, Thomann E, Waymire E, Wood B. Solute transport across an interface: a Fickian theory for skewness in breakthrough curves. Water Resour Res 2010;46(7). http://dx.doi.org/10.1029/2009WR008258.
[3] Aubeneau A, Hanrahan B, Bolster D, Tank J. Substrate size and heterogeneity control anomalous transport in small streams. Geophys Res Lett 2014. http://dx.doi.org/10.1002/2014GL061838.
[4] Aubeneau AF, Drummond J, Schumer R, Bolster D, Tank J, Packman A. Effects of benthic and hyporheic reactive transport on breakthrough curves. Freshwater Sci 2014. http://dx.doi.org/10.1086/680037.
[5] Baeumer B, Benson DA, Meerschaert MM, Wheatcraft SW. Subordinated advection–dispersion equation for contaminant transport. Water Resour Res 2001;37(6):1543–50. http://dx.doi.org/10.1029/2000WR900409.
[6] Battin TJ, Kaplan LA, Newbold JD, Hansen CM. Contributions of microbial biofilms to ecosystem processes in stream mesocosms. Nature 2003;426(6965):439–42. http://dx.doi.org/10.1038/nature02152.
[7] Bear J. Dynamics of fluids in porous media. Courier Dover Publications; 2013. ISBN-10: 0486656756.
[8] Benson DA, Meerschaert MM. A simple and efficient random walk solution of multi-rate mobile/immobile mass transport equations. Adv Water Resour 2009;32(4):532–9. http://dx.doi.org/10.1016/j.advwatres.2009.01.002.
[9] Berkowitz B, Cortis A, Dentz M, Scher H. Modeling non-Fickian transport in geological formations as a continuous time random walk. Rev Geophys 2006;44(2). http://dx.doi.org/10.1029/2005RG000178.
[10] Bhattacharya R, Gupta VK, Sposito G. On the stochastic foundations of the theory of water flow through unsaturated soil. Water Resour Res 1976;12(3):503–12. http://dx.doi.org/10.1029/WR012i003p00503.
[11] Bolster D, Meheust Y, Borgne TL, Bouquain J, Davy P. Modeling preasymptotic transport in flow with significant inertial and trapping effects – the importance of velocity correlations and a spatial markov model. Adv Water Resour 2014;70(89–103). http://dx.doi.org/10.1016/j.advwatres.2014.04.014.
[12] Bolster D, Valdés-Parada FJ, LeBorgne T, Dentz M, Carrera J. Mixing in confined stratified aquifers. J Contaminant Hydrol 2011;120:198–212. http://dx.doi.org/10.1016/j.jconhyd.2010.02.003.
[13] Boso F, Bellin A, Dumbser M. Numerical simulations of solute transport in highly heterogeneous formations: a comparison of alternative numerical schemes. Adv Water Resour 2013;52:178–89. http://dx.doi.org/10.1016/j.advwatres.2012.08.006.
[14] Cardenas MB. Surface water-groundwater interface geomorphology leads to scaling of residence times. Geophys Res Lett 2008;35(8). http://dx.doi.org/10.1029/2008GL033753.
[15] Chakraborty P, Meerschaert MM, Lim CY. Parameter estimation for fractional transport: a particle-tracking approach. Water Resour Res 2009;45(10). http://dx.doi.org/10.1029/2008WR007577.
[16] Cole JJ, Prairie YT, Caraco NF, McDowell WH, Tranvik LJ, Striegl RG, Duarte CM, Kortelainen P, Downing JA, Middelburg JJ, et al. Plumbing the global carbon cycle: integrating inland waters into the terrestrial carbon budget. Ecosystems 2007;10(1):172–85. http://dx.doi.org/10.1007/s10021-006-9013-8.
[17] Covino TP, McGlynn BL. Stream gains and losses across a mountain-to-valley transition: impacts on watershed hydrology and stream water chemistry. Water Resour Res 2007;43(10). http://dx.doi.org/10.1029/2006WR005544.
[18] De Anna P, Le Borgne T, Dentz M, Tartakovsky AM, Bolster D, Davy P. Flow intermittency, dispersion, and correlated continuous time random walks in porous media. Phys Rev Lett 2013;110(18):184502. http://dx.doi.org/10.1103/PhysRevLett.110.184502.
[19] Delay F, Ackerer P, Danquigny C. Simulating solute transport in porous or fractured formations using random walk particle tracking. Vadose Zone J 2005;4(2):360–79. http://dx.doi.org/10.2136/vzj2004.0125.
[20] Ding M, Yang W. Distribution of the first return time in fractional brownian motion and its application to the study of on–off intermittency. Phys Rev E 1995;52(1):207. http://dx.doi.org/10.1103/PhysRevE.52.207.
[21] Drummond J, Covino T, Aubeneau A, Leong D, Patil S, Schumer R, Packman A. Effects of solute breakthrough curve tail truncation on residence time estimates: a synthesis of solute tracer injection studies. J Geophys Res:

Biogeosci (2005–2012) 2012;117(G3). http://dx.doi.org/10.1029/2012JG002019.
[22] Feller W. An introduction to probability theory and its applications, vol. 2. John Wiley & Sons; 2008. ISBN-10: 0471257095.
[23] Fischer HB. Longitudinal dispersion and turbulent mixing in open-channel flow. Annu Rev Fluid Mech 1973;5(1):59–78. http://dx.doi.org/10.1146/annurev.fl.05.010173.000423.
[24] Fischer HB. Mixing in inland and coastal waters. Academic press; 1979. ISBN-10: 0122581504.
[25] Haggerty R, Wondzell SM, Johnson MA. Power-law residence time distribution in the hyporheic zone of a 2nd-order mountain stream. Geophys Res Lett 2002;29(13):18-1. http://dx.doi.org/10.1029/2002GL014743.
[26] Harvey JW, Fuller CC. Effect of enhanced manganese oxidation in the hyporheic zone on basin-scale geochemical mass balance. Water Resour Res 1998;34(4):623–36. http://dx.doi.org/10.1029/97WR03606.
[27] Heslop SE, Allen CM. Modelling contaminant dispersion in the river severn using a random-walk model. J Hydraul Res 1993;31(3):323–31. http://dx.doi.org/10.1080/00221689309498829.
[28] LaBolle EM, Fogg GE, Tompson AF. Random-walk simulation of transport in heterogeneous porous media: local mass-conservation problem and implementation methods. Water Resour Res 1996;32(3):583–93. http://dx.doi.org/10.1029/95WR03528.
[29] Le Borgne T, Bolster D, Dentz M, Anna P, Tartakovsky A. Effective pore-scale dispersion upscaling with a correlated continuous time random walk approach. Water Resour Res 2011;47(12). http://dx.doi.org/10.1029/2011WR010457.
[30] Le Borgne T, Dentz M, Carrera J. Lagrangian statistical model for transport in highly heterogeneous velocity fields. Phys Rev Lett 2008;101(9):090601. http://dx.doi.org/10.1103/PhysRevLett.101.090601.
[31] Leopold LB, Leopold LB. Fluvial processes in geomorphology. Courier Dover Publications; 1995. ISBN-10: 0486685888.
[32] Meerschaert MM, Scheffler H-P. Limit distributions for sums of independent random vectors: heavy tails in theory and practice, vol. 321. John Wiley & Sons; 2001. ISBN-978-0-471-35629-5.
[33] Metzler R, Klafter J. The restaurant at the end of the random walk: recent developments in the description of anomalous transport by fractional dynamics. J Phys A: Math Gen 2004;37(31):R161. http://dx.doi.org/10.1088/0305-4470/37/31/R01.
[34] Mulholland PJ, Helton AM, Poole GC, Hall RO, Hamilton SK, Peterson BJ, Tank JL, Ashkenas LR, Cooper LW, Dahm CN, et al. Stream denitrification across biomes and its response to anthropogenic nitrate loading. Nature 2008;452(7184):202–5. http://dx.doi.org/10.1038/nature06686.
[35] Peterson BJ, Wollheim WM, Mulholland PJ, Webster JR, Meyer JL, Tank JL, Marti E, Bowden WB, Valett HM, Hershey AE, et al. Control of nitrogen export from watersheds by headwater streams. Science 2001;292(5514):86–90. http://dx.doi.org/10.1126/science.1056874.
[36] Risken H. The Fokker–Planck equation, methods of solution and applications. Springer; 1984. ISBN-978-3-642-61544-3.
[37] Salamon P, Fernàndez-Garcia D, Gómez-Hernández JJ. A review and numerical assessment of the random walk particle tracking method. J Contaminant Hydrol 2006;87(3):277–305. http://dx.doi.org/10.1016/j.jconhyd.2006.05.005.
[38] Taylor G. Dispersion of soluble matter in solvent flowing slowly through a tube. Proc Roy Soc Lond Ser A 1953;219:186–203. http://dx.doi.org/10.1098/rspa.1953.0139.
[39] Wang L, Cardenas MB, Deng W, Bennett PC. Theory for dynamic longitudinal dispersion in fractures and rivers with poiseuille flow. Geophys Res Lett 2012;39(5). http://dx.doi.org/10.1029/2011GL050831.
[40] Worman A, Packman AI, Johansson H, Jonsson K. Effect of flow-induced exchange in hyporheic zones on longitudinal transport of solutes in streams and rivers. Water Resour Res 2002;38(1):2-1. http://dx.doi.org/10.1029/2001WR000769.